Comparative evaluation of ^{111}In-labeled NOTA-conjugated affibody molecules for visualization of HER3 expression in malignant tumors

KEN G. ANDERSSON[1], MARIA ROSESTEDT[2], ZOHREH VARASTEH[2], MAGDALENA MALM[1], MATTIAS SANDSTRÖM[3], VLADIMIR TOLMACHEV[4], JOHN LÖFBLOM[1], STEFAN STÅHL[1] and ANNA ORLOVA[2]

[1]Division of Protein Technology, KTH Royal Institute of Technology, Stockholm; [2]Preclinical PET Platform, [3]Nuclear Medicine and PET, [4]Institute of Immunology, Genetic and Pathology, Uppsala University, Uppsala, Sweden

Received February 17, 2015; Accepted March 20, 2015

DOI: 10.3892/or.2015.4046

Abstract. Expression of human epidermal growth factor receptor type 3 (HER3) in malignant tumors has been associated with resistance to a variety of anticancer therapies. Several anti-HER3 monoclonal antibodies are currently under pre-clinical and clinical development aiming to overcome HER3-mediated resistance. Radionuclide molecular imaging of HER3 expression may improve treatment by allowing the selection of suitable patients for HER3-targeted therapy. Affibody molecules are a class of small (7 kDa) high-affinity targeting proteins with appreciable potential as molecular imaging probes. In a recent study, we selected affibody molecules with affinity to HER3 at a low picomolar range. The aim of the present study was to develop an anti-HER3 affibody molecule suitable for labeling with radiometals. The HEHEHE-Z08698-NOTA and HEHEHE-Z08699-NOTA HER3-specific affibody molecules were labeled with indium-111 (^{111}In) and assessed *in vitro* and *in vivo* for imaging properties using single photon emission computed tomography (SPECT). Labeling of HEHEHE-Z08698-NOTA and HEHEHE-Z08699-NOTA with ^{111}In provided stable conjugates. *In vitro* cell tests demonstrated specific binding of the two conjugates to HER3-expressing BT-474 breast carcinoma cells. In mice bearing BT-474 xenografts, the tumor uptake of the two conjugates was receptor-specific. Direct *in vivo* comparison of ^{111}In-HEHEHE-Z08698-NOTA and ^{111}In-HEHEHE-Z08699-NOTA demonstrated that the two conjugates provided equal radioactivity uptake in tumors, although the tumor-to-blood ratio was improved for ^{111}In-HEHEHE-Z08698-NOTA [12±3 vs. 8±1, 4 h post injection (p.i.)] due to more efficient blood clearance. ^{111}In-HEHEHE-Z08698-NOTA is a promising candidate for imaging of HER3-expression in malignant tumors using SPECT. Results of the present study indicate that this conjugate could be used for patient stratification for anti-HER3 therapy.

Correspondence to: Dr Anna Orlova, Preclinical PET Platform, Uppsala University, Dag Hammarskjöldsv 14C, 751 83 Uppsala, Sweden
E-mail: anna.orlova@pet.medchem.uu.se

Key words: NOTA, indium-111, affibody molecules, HER3, molecular imaging

Introduction

The human epidermal growth factor receptor type 3 (HER3 or ErbB3) has recently attracted attention as a molecular target for anticancer therapy (1-3). HER3 has no tyrosine kinase activity of its own and participates in signaling by heterodimerization with other members of the HER family (4). One of the mechanisms behind acquired resistance of breast cancer patients to HER2-targeting therapies may be due to the upregulation of HER3 and hyperactivation of its signaling (5,6). In addition, HER3 has been shown to be involved in resistance to hormone therapy in breast cancer (7). Furthermore, HER3 expression in ovarian cancer is associated with more aggressive disease; in lung cancer, with resistance to tyrosine kinase-inhibiting therapy; and in prostate cancer HER3 expression may drive tumor cell growth in hormone refractory cancer (1). Thus, there is a strong rationale for the development of pharmaceuticals specifically targeting HER3. Besides monoclonal antibodies, HER3-targeting antisense oligonucleotides and scaffold proteins are under pre-clinical and early clinical development (3,8,9).

The clinical implementation of anti-HER3 therapy is a challenge. Treatment should be initiated at onset of HER3 overexpression to avoid overtreatment. As HER3 overexpression often occurs as a response to therapy, the samples from primary tumors would not be informative. Serial biopsies are undesirable due to invasiveness of the procedure and HER3 overexpression may not be synchronous in all the metastases that occur. The use of radionuclide molecular imaging is a useful strategy since it is non-invasive, repeatable and provides whole-body information.

Prerequisites for the successful application of molecular imaging are high specificity and sensitivity. Although radiolabeling of available therapeutic anti-HER3 monoclonal antibodies is an approach to the development of imaging probes, it is difficult to obtain a high sensitivity and specificity

in this manner. Anti-HER3 antibody (10) and F(ab')2 antibody fragments (11) were recently evaluated for positron emission tomography (PET) imaging in a preclinical setting. Slow clearance of antibodies from blood results in a high background even several days after injection, reducing imaging contrast and sensitivity. Additionally, bulky immunoglobulins with a molecular weight of >45 kDa tend to accumulate non-specifically in tumors due to an 'enhanced permeability and retention' (EPR) effect (12). This may cause false-positive findings, i.e., specificity of antibody-mediated imaging is low. A possible solution is the use of smaller imaging agents, which provide rapid extravasation and diffusion into the extracellular space, rapid clearance of unbound tracer, and exclude the EPR effect.

Previously, we demonstrated the feasibility of radionuclide imaging of HER3 expression *in vivo* (murine models) using a ^{99m}Tc-labeled HER3-antagonistic affibody molecule $^{99m}Tc(CO)_3$-HEHEHE-Z08699 (13). Affibody molecules are small (7 kDa) scaffold proteins that are selected using molecular display techniques for high-affinity binding to different target proteins (14). Affibody molecules have demonstrated the ability of imaging of HER2 expression in breast cancer patients (15,16).

HER3-targeting affibody molecules Z08698 and Z08699 have been selected and demonstrate high affinities to HER3 (50 and 21 pM, respectively) (9). Such high affinities are important for the imaging of molecular targets with a relatively low tumor expression. Z08698 and Z08699 were also found to have high affinity to the murine counterpart of HER3, mErbM3, rendering mice an adequate model for the evaluation of imaging properties (13).

The aim of this study was the development of a HER3 imaging agent labeled with radiometals suitable for single photon emission computed tomography (SPECT) and PET.

Engineering of a unique cysteine into affibody molecules provides site-specific conjugation of the chelator, resulting in well-defined products with reproducible biodistribution properties. Findings regarding affibody molecules suggested that placement of a cysteine at the C-terminus is convenient, as this provides a maximum distance from a binding site and minimizes possible interference of the chelator with the molecular recognition (17,18). The use of the NOTA chelator (2,2',2''-(1,4,7-triazonane-1,4,7-triyl)triacetic acid) provides stable labeling with ^{111}In for SPECT, and with ^{68}Ga, ^{64}Cu or ^{18}F (using aluminum monofluoride ^{18}F-AlF chemistry) for PET. Previously, we showed that placement of a HEHEHE-tag (histidyl-glytamyl-histidyl-glytamyl-histidyl-glytamyl) at the N-terminus permits immobilized metal ion affinity chromatography (IMAC) purification of affibody molecules and improves their biodistribution by reducing hepatic uptake (13,19). Bearing these considerations in mind, we generated two anti-HER3 affibody molecules with the HEHEHE-tag at the N-terminus and NOTA chelator at the C-terminus (i.e., HEHEHE-Z-NOTA) (Fig. 1).

Investigations on factors influencing imaging using HER2-targeting affibody molecules have demonstrated that low picomolar affinity is essential for the imaging of targets with low expression, such as HER3 (20). Previous findings have also demonstrated that small changes in amino acid composition can modify off-target interactions and affect blood clearance

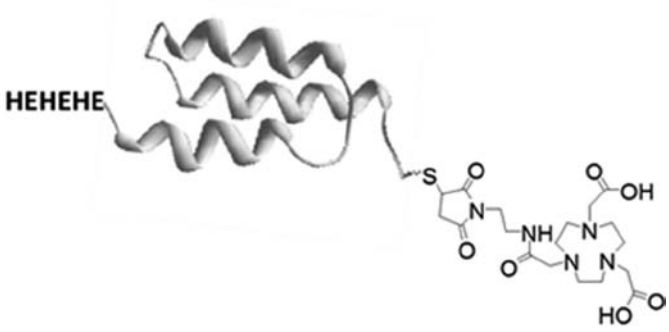

Figure 1. Structure of affibody-based imaging agents. Anti-HER3 affibody molecule (58 amino acids, ~7 kDa) coupled to a HEHEHE-tag (histidyl-glytamyl-histidyl-glytamyl-histidyl-glytamyl) at the N-terminus and site-specifically conjugated with a NOTA chelator to a C-terminal cysteine for labeling with indium-111.

rate and hepatic uptake (20). Thus high affinity is not the only parameter to be considered for the selection of affibody molecules for imaging, and evaluation of several variants with approximately equal affinity may prove useful in selecting an agent with the most suitable *in vivo* properties.

Findings obtained showed that targeting of HER3 and other tyrosine kinases with an expression pattern similar to that of HER3 (endogenous expression in healthy tissue, e.g., IGF-1R) suggested that imaging contrast could be improved at later time-points (i.e., at 24 h p.i.) (13,21). Thus, ^{111}In was used as a label whose half-life permits studying biodistribution at the day of injection and during the following day. The targeting properties of ^{111}In-HEHEHE-Z08698-NOTA and ^{111}In-HEHEHE-Z08699-NOTA were compared *in vitro* and *in vivo* in nude mice bearing HER3-expressing BT-474 breast carcinoma xenografts.

Materials and methods

High-quality Milli-Q water (resistance >18 MΩ/cm) was used to prepare the solutions. [^{111}In]-indium chloride was purchased from Covidien, Ltd. (Dublin, Ireland). Cells used during the *in vitro* experiments were detached using trypsin-EDTA solution (0.05% trypsin, 0.02% EDTA in buffer; Biochrom AG, Berlin, Germany). Radioactivity was measured using an automated gamma-counter with a 3-inch NaI(Tl) detector (1480 Wizard; Wallac Oy, Turku, Finland). The purity of radiolabeled affibody molecules was determined by radio ITLC (150-771 Dark Green, Tec-Control Chromatography strips from Biodex Medical Systems) and cross-validated by sodium dodecyl sulfate polyacrylamide gel electrophoresis (SDS-PAGE). The distribution of radioactivity along the thin layer chromatography strips was measured on a Cyclone Storage Phosphor System and analyzed using the OptiQuant image analysis software (Perkin-Elmer, Waltham, MA, USA).

For the *in vitro* and *in vivo* experiments, the HER3-expressing BT-474 breast carcinoma cell line [American Type Tissue Culture Collection (ATCC) via LGC Promochem, Borås, Sweden] was used. Animal experiments were planned and performed in accordance with national legislation on protection of laboratory animals and were approved by the Ethics Committee for Animal Research in Uppsala, Sweden.

Data on the cell uptake and biodistribution were assessed by an unpaired, two-tailed t-test using GraphPad Prism (version 4.00 for Windows GraphPad Software) to determine significant differences ($P<0.05$).

Production, purification, NOTA-conjugation and analysis of affibody molecules. Production of Z08698 and Z08699 was previously described (9,13). In the present study, the DNA sequences encoding Z08698 and Z08699 were amplified using polymerase chain reaction (PCR) with primers incorporating a HEHEHE-tag (N-terminal) and cysteine (C-terminal). Coupling of NOTA chelator was performed as previously described (22). The NOTA-conjugated proteins were subsequently purified using a 1200 series HPLC system in a Zorbax C18 semi-preparative column (Agilent Technologies, Santa Clara, CA, USA). The molecular masses of the purified proteins were confirmed using a 6520 Accurate-Mass Q-TOF LC/MS (Agilent Technologies). The purity of the NOTA-conjugated affibody molecules was determined using an analytical column Zorbax 300B-C18 (Agilent Technologies) on 1200 series RP-HPLC (Agilent Technologies). The secondary structure content, thermal stability and refolding capacity was analyzed using circular dichroism (CD) spectroscopy on a Jasco-810 (Jasco Inc., Easton, MD, USA). Affinities to human ErbB3-FC (R&D Systems, Minneapolis, MN, USA) were determined on a BiaCore 3000 system (GE Healthcare, Pittsburgh, PA, USA).

Labeling of HEHEHE-Z08698-NOTA and HEHEHE-Z08699-NOTA with ^{111}In. For labeling, ^{111}In-HEHEHE-Z08698-NOTA or ^{111}In-HEHEHE-Z08699-NOTA (40 μg, 6 nmol, in 100 μl 0.2 M ammonium acetate, pH 5.5) was incubated with 54 μl ^{111}In-chloride solution (40 MBq) at 85˚C for 40 min. The reaction mixture was obtained and analyzed by radio-ITLC (instant thin-layer chromatography) eluted with 0.2 M citric acid, pH 2.0. To cross-validate the ITLC, an SDS-PAGE analysis (200 V constant, NuPAGE 4-16% Bis-Tris gel; Invitrogen AB) was performed. To ensure high radiochemical purity, the conjugates were purified using disposable NAP-5 columns (GE Healthcare) according to the manufacturer's instructions.

An EDTA-challenge was performed to evaluate the labeling stability of conjugates [500-fold molar excess of the tetrasodium salt of ethylenediaminetetraacetic acid (EDTA) solution in water, 2 h at room temperature]. The samples were analyzed using radio-ITLC. To evaluate stability of the conjugates in serum, labeled conjugates were incubated at 37˚C in fetal bovine serum (5 μg in 200 μl PBS diluted with 200 μl serum). At 4- and 24-h incubation, the samples were analyzed using SDS-PAGE. For the control, labeled conjugates were incubated under the same conditions in PBS. No release of free ^{111}In or transchelation to serum proteins was detected (data not shown).

Real-time ligand-binding kinetics, and K_D determination for ^{111}In-HEHEHE-Z08698-NOTA and ^{111}In-HEHEHE-Z08699-NOTA on BT-474 cells. The binding of ^{111}In-HEHEHE-Z08698-NOTA and ^{111}In-HEHEHE-Z08699-NOTA on BT-474 cells was measured in real-time at room temperature using LigandTracer Yellow (Ridgeview Instruments AB, Vänge, Sweden) as previously described (23). The radioligand concentrations of 0.2 and 2 nM were used. These concentrations were selected to receive a clear increase in signal by addition of the second concentration. Uptake was monitored for 105 min and retention for 960 min. Interaction analysis and calculation of equilibrium dissociation constant (K_D) was performed with TracerDrawer software (Ridgeview Instruments AB).

In vitro specificity of ^{111}In-HEHEHE-Z08698-NOTA and ^{111}In-HEHEHE-Z08699-NOTA to HER3-expressing cells. *In vitro* experiments were performed in triplicate. For experiments $1x10^6$ BT-474 cells/dish were seeded the day prior to the experiment.

An *in vitro* specificity test was performed as previously described (24). Briefly, a solution of radiolabeled affibody molecules (at 0.1 nM) was added to the cell plates. For blocking, 5 nM of non-labeled affibody molecule was added 15 min before the radiolabeled conjugates to saturate the receptors in half of the dishes. The cells were incubated for 1 h at 37˚C. Thereafter, the medium was collected and the cells were detached by trypsin-EDTA solution. The samples were measured on radioactivity content to enable calculation of the fraction of cell-bound radioactivity.

In vivo studies. To evaluate targeting of HER3-expressing tumors *in vivo*, mice bearing BT-474 breast carcinoma xenografts were used. Ten million BT-474 cells were implanted in 50% Matrigel in Balb/c nu/nu female mice pre-implanted with estradiol pellets (0.025 mg/day, 20 days; Innovative Research of America, Sarasota, FL, USA) and used 3 weeks after implantation. Tumor size at initiation of the experiment was 0.6±0.3 g. Mice (3-4 per group) were intravenously injected with ^{111}In-HEHEHE-Z08698-NOTA or ^{111}In-HEHEHE-Z08699-NOTA (1 μg/30 kBq in 100 μl PBS). The animals were sacrificed at 1, 4, 8 and 24 h p.i. by injection of a lethal dose of anesthesia [20 μl of Ketalar Rompun per gram body weight: Ketalar (50 mg/ml; Pfizer), 10 mg/ml; Rompun, (20 mg/ml; Bayer] followed by heart puncture and exsanguination with a syringe rinsed with heparin (5000 IE/ml; Leo Pharma). Tumors and samples of blood, lung, liver, spleen, stomach, small intestines, kidney, salivary gland, muscle and bone were collected, weighed and their radioactivity was measured. The data were corrected for background. Tissue uptake was calculated as %IA/g (percent of injected radioactivity per gram).

To evaluate if uptake in tumors and mErbB3-expressing organs and tissues was saturable, labeled affibody conjugates were intravenously injected in a group of mice with injected protein dose adjusted by dilution with non-labeled affibody molecule to 70 μg per mouse. Biodistribution was performed 4 h p.i. as described above.

Imaging studies. The study was performed to obtain visual confirmation of the biodistribution data. Tumor-bearing mice were injected with 0.8 MBq ^{111}In-HEHEHE-Z08698-NOTA (1 μg) and ^{111}In-HEHEHE-Z08699-NOTA (1 and 70 μg). At 4 h p.i., the animals were euthanized and the urinary bladder was excised post-mortem to improve image quality. Static planar imaging of the three mice was performed simultaneously using a GE Infinia gamma camera equipped with a MEGP (medium energy general purpose) collimator. Static images (20 min) of the three animals were obtained with a zoom factor of 3 in a 256x256 matrix.

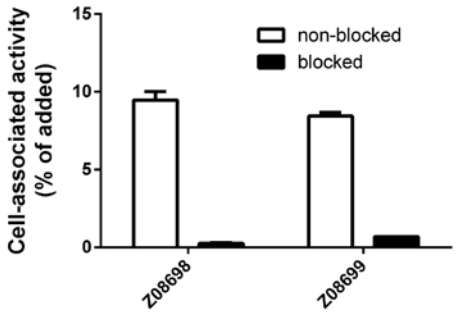

Figure 2. *In vitro* characterization of ^{111}In-HEHEHE-Z08698-NOTA and ^{111}In-HEHEHE-Z08699-NOTA. Binding specificity of labeled conjugates to HER3-expressing BT-474 cells. Data are presented as mean values of 3 ± SD.

Statistical analysis. Data are presented as mean ± SD.

Results

Production, purification and analysis of conjugates. The affibody molecules were expressed in *E. coli* and purified using heat-induced precipitation of host proteins. Correct size and sufficient purity for conjugation was confirmed using SDS-PAGE (data not shown). Mass-spectrometry analysis revealed that the two binders had the expected molecular weight after conjugation to the NOTA chelator at the C-terminal cysteine using maleimide chemistry [HEHEHE-Z08698-NOTA-8149.55 (8149) and HEHEHE-Z08699-NOTA-8112.39 (8112) Da]. Analysis using RP-HPLC showed purities of 95.6 and 96.6% for HEHEHE-Z08698-NOTA and HEHEHE-Z08699-NOTA, respectively. Circular dichroism (CD) spectra verified expected α-helical secondary structure content, indicating that correct folding into a three-helical bundle, and variable temperature measurement (VTM) at 221 nm revealed melting temperatures (T_m) of 65˚C and 63˚C for Z08698 and Z08699, respectively. CD measurements following VTM treatment showed no loss of helical content, demonstrating complete refolding upon lowering the temperature after heat-induced denaturation. According to the SPR analysis, dissociation constants for binding to HER3 were 45 and 77 pM for HEHEHE-Z08698-NOTA and HEHEHE-Z08699-NOTA, respectively.

Labeling and in vitro stability. The average yield of ^{111}In-HEHEHE-Z08698-NOTA was 95±3%, and that of ^{111}In-HEHEHE-Z08699-NOTA was 96.2±0.5%. Simple purification using disposable size-exclusion columns provided a radiochemical purity of >98%. A specific activity of 8 GBq/μmol was obtained routinely during labeling. The two conjugates were stable under EDTA-challenge for 2 h and in fetal bovine serum for 24 h at 37˚C.

In vitro receptor binding. An *in vitro* cell binding assay showed that the two affibody molecules bound to HER3-positive BT-474 cells. Moreover, saturation of the receptors by pre-incubation with non-labeled affibody molecules significantly decreased the binding of the radiolabeled conjugates, demonstrating that the interactions were specific (Fig. 2).

According to the analysis of real-time ligand-binding kinetics data, the calculated K_D values for ^{111}In-HEHEHE-Z08698-NOTA and ^{111}In-HEHEHE-Z08699-NOTA were in the picomolar range (5.4±0.4 and 4.2±0.4 pM, respectively) (data not shown).

In vivo studies. The two conjugates demonstrated specific binding *in vivo* to HER3 (BT-474 xenografts) and to mErbB3 (Fig. 3). Uptake of radioactivity in BT-474 xenografts and the mErbB3-expressing organs and tissues was significantly reduced when 70 μg of affibody molecule was injected compared to 1 μg. Reduction in radioactivity uptake in liver was more pronounced for the Z08699 variant. At the same time, significantly increased uptake was identified in kidneys for the two conjugates.

Biodistribution over time of ^{111}In-HEHEHE-Z08698-NOTA and ^{111}In-HEHEHE-Z08699-NOTA in BT-474 xenograft-bearing mice is presented in Tables I and II. The overall pattern of radioactivity distribution in tumors and normal organs was similar for the two conjugates. The tumor

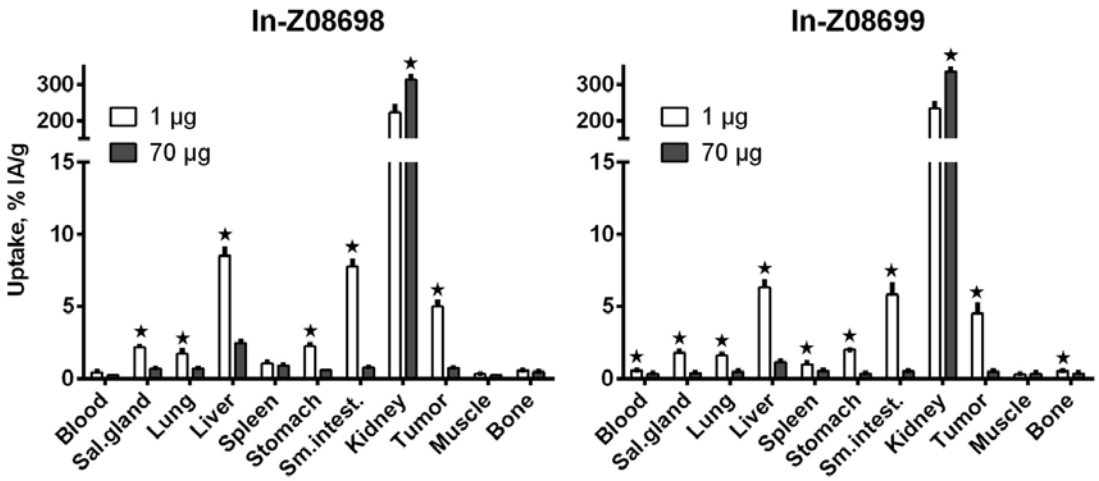

Figure 3. *In vivo* binding specificity of ^{111}In-HEHEHE-Z08698-NOTA and ^{111}In-HEHEHE-Z08699-NOTA, BT-474 xenografts, 4 h p.i. Results are presented as a percentage of injected activity per gram of tissue (% IA/g) as average of 4 ± SD. Statistical significance in the tissue uptake between the groups (stars) according to the Student's t-test, P<0.05. Sal.gland, salivary glands; Sm.intest, small intestines.

Table I. Biodistribution of ^{111}In-HEHEHE-Z08698-NOTA and ^{111}In-HEHEHE-Z08699-NOTA in BT-474 tumor-bearing Balb/c nu/nu mice.

	^{111}In-HEHEHE-Z08698-NOTA				^{111}In-HEHEHE-Z08699-NOTA			
Organ	1 h	4 h	8 h	24 h	1 h	4 h	8 h	24 h
Blood	0.95±0.04	0.4±0.1	0.34±0.05	0.24±0.02	1.10±0.09[b]	0.56±0.06	0.42±0.02[b]	0.20±0.02
Salivary gland	2.97±0.08	2.2±0.2	1.9±0.2	1.4±0.5	2.5±0.1	1.8±0.2	1.5±0.4	0.9±0.3
Lung	2.1±0.5	1.7±0.5	1.1±0.2	0.73±0.04	2.3±0.2	1.6±0.3	1.2±0.1	0.8±0.3
Liver	7.7±0.8[a]	8±1[a]	7.5±0.4[a]	4.9±0.2[a]	6.0±0.4	6.3±0.7	4.7±0.6	3.0±0.1
Spleen	1.0±0.2[a]	1.1±0.2	1.0±0.1	1.01±0.05[a]	0.91±0.02	1.0±0.2	0.92±0.05	0.71±0.04
Stomach	3.0±0.4	2.2±0.3	1.8±0.2[a]	1.51±0.09[a]	2.9±0.6	1.99±0.07	1.3±0.1	0.92±0.01
Small intestine	12±5	7.8±0.8[a]	5.2±0.9	5±2	9±2	6±1	5±2	2.1±0.7
Kidney	187±9	223±33	182±24	188±24	194±14	233±28	244±23[b]	195±11
Tumor	5.1±0.4	5.0±0.6	4.0±0.2	3.7±0.2[a]	4.7±0.8	5±1	3.9±0.4	2.4±0.2
Muscle	0.37±0.06	0.32±0.08	0.21±0.05	0.3±0.2	0.34±0.06	0.29±0.06	0.3±0.1	0.19±0.08
Bone	0.61±0.05	0.57±0.07	0.34±0.04	0.37±0.07	0.7±0.2	0.53±0.07	0.53±0.06	0.37±0.04

Results are presented as an average of 4 ± SD. [a]Uptake of ^{111}In-HEHEHE-Z08698-NOTA and [b]uptake of ^{111}In-HEHEHE-Z08699-NOTA was significantly higher ($P<0.05$) at this time-point.

Table II. Tumor-to-organ ratios of ^{111}In-HEHEHE-Z08698-NOTA and ^{111}In-HEHEHE-Z08699-NOTA in BT-474 tumor-bearing Balb/c nu/nu mice.

	^{111}In-HEHEHE-Z08698-NOTA				^{111}In-HEHEHE-Z08699-NOTA			
Organ	1 h	4 h	8 h	24 h	1 h	4 h	8 h	24 h
Blood	5.3±0.4	12±3[a]	12±2	15.5±0.7[a]	4.3±0.8	8±1	9±1	11.8±0.1
Salivary gland	1.7±0.2	2.3±0.3	2.1±0.1	3±1	1.9±0.4	2.5±0.7	2.8±0.9	3.0±1.0
Lung	2.5±0.6	3.0±0.4	3.6±0.7	5.1±0.4	2.0±0.3	2.9±0.8	3.2±0.4	3±1
Liver	0.66±0.06	0.59±0.06	0.53±0.01	0.75±0.07	0.8±0.2	0.7±0.2	0.8±0.1[b]	0.80±0.08
Spleen	5.1±0.6	4.7±0.5	4.1±0.4	3.7±0.3	5.2±0.8	4.5±0.4	4.3±0.5	3.4±0.2
Stomach	1.7±0.2	2.3±0.2	2.3±0.3	2.45±0.08	1.7±0.4	2.3±0.6	3.0±0.6	2.6±0.3
Small intestine	0.5±0.2	0.65±0.09	0.77±0.10	0.8±0.3	0.5±0.2	0.8±0.2	0.8±0.1	1.2±0.3
Muscle	14±2	16±4	20±6	16±8	14±4	16±7	15±6	14±4
Bone	8±1	8.9±0.5	12±2[a]	10±3	7±1	9±2	7.5±0.9	6.3±0.2

Results are presented as an average of 4 ± SD. [a]Value for ^{111}In-HEHEHE-Z08698-NOTA and [b]value for ^{111}In-HEHEHE-Z08699-NOTA was significantly higher ($P<0.05$) at this time-point.

uptake of radioactivity exceeded radioactivity concentration in blood at 1 h p.i. and the tumor-to-blood ratio increased over time (Table I). The uptake of radioactivity in tumors was higher than that in organs with mErbB3 expression (salivary glands, lungs and stomach). On the other hand, the uptake of radioactivity in liver and small intestine tissue was higher than that in tumors. The uptake of radioactivity in tissues without mErbB3 expression (spleen, muscle and bone) was low. The main excretion pathway was renal for the two conjugates with substantial retention of radioactivity in kidneys. Differences in the biodistribution pattern between ^{111}In-HEHEHE-Z08698-NOTA and ^{111}In-HEHEHE-Z08699-NOTA were observed. ^{111}In-HEHEHE-Z08698-NOTA demonstrated more rapid blood clearance, better radioactivity retention in tumors, higher tumor-to-blood ratio at 24 h p.i., but higher uptake of radioactivity in liver. The tumor-to-muscle ratios were in the range of 15-20 and the tumor-to-bone ratios, in the range of 6-12 (Table II). Tumor-to-liver ratios were <1, and the tumor-to-intestine ratio was >1 for ^{111}In-HEHEHE-Z08699-NOTA at 24 h p.i. (Table II).

Gamma-camera images (Fig. 4) confirmed the major findings of the biodistribution study. The two conjugates visualized HER3-expressing xenografts at 4 h p.i. It was clearly demonstrated that co-injection of 70 μg of non-labeled Z08699 decreased the uptake of radioactivity in the xenograft. In agreement with the biodistribution data, the radioactivity uptake in kidneys dominated the images and radioactivity uptake in liver was at least on the same level as in the tumors.

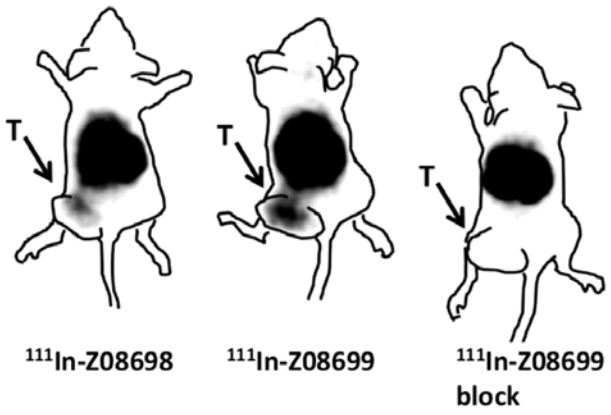

Figure 4. Gamma-camera image of mice bearing HER3-expressing BT-474 xenografts at 4 h p.i. of conjugates.

It was also confirmed that blood clearance occurred more rapidly for ^{111}In-HEHEHE-Z08698-NOTA, resulting in lower background radioactivity.

Discussion

Elucidation of the role of HER3 in cancer resistance to different types of treatments has resulted in the development of HER3-targeting therapies. Imaging may be a valuable clinical tool for the stratification of patients for such therapies, making treatment more personalized. Previously, we demonstrated the feasibility of imaging of HER3-expressing xenografts using a ^{99m}Tc-labeled anti-HER3 HEHEHE-Z08698 affibody molecule (13). That investigation initiated a series of studies focused on the development of affibody-based HER3-imaging agents suitable for PET and SPECT applications. To achieve that aim, a NOTA chelator, site-specifically conjugated to a C-terminal cysteine of the affibody molecule was selected. In a new HEHEHE-Z-NOTA format tested for two variants, Z08698 and Z08699, the affibody molecules retained their low picomolar affinity to HER3. However, the altered format was found to have some effect on the mutual affinities. The dissociation constant of HEHEHE-Z08698-NOTA (45 pM) was lower than that of HEHEHE-Z08699-NOTA (77 pM), while the opposite relationship was observed for the parental affibody molecules Z08698 (50 pM) and Z08699 (21 pM). The two conjugates retained a capacity for high-fidelity refolding after heating, which is essential as labeling using macrocyclic chelators requires relatively harsh temperature conditions. Labeling of conjugates was performed at elevated temperatures (85˚C) that provided stable labeling of ^{111}In-HEHEHE-Z08698-NOTA and ^{111}In-HEHEHE-Z08699-NOTA. However, the two conjugates demonstrated preserved binding specificity to HER3-expressing BT-474 breast cancer cells after labeling.

The two conjugates demonstrated saturable binding to HER3-expressing breast cancer xenografts *in vivo*, which suggests target-specific uptake. Of note, saturable uptake was also demonstrated in mErbB3-expressing murine tissues (Fig. 3). Expression of a molecular target in normal tissues may appreciably affect imaging, and cross-reactivity of affibody molecules with the murine counterpart makes the animal model adequate for assessment of imaging properties.

Uptake of conjugates in tumor xenografts did not differ significantly between ^{111}In-HEHEHE-Z08698-NOTA and ^{111}In-HEHEHE-Z08699-NOTA at earlier time points (1-8 h p.i.). However, ^{111}In-HEHEHE-Z08698-NOTA had improved tumor retention of radioactivity at 24 h p.i. The main difference between the conjugates was in their uptake in normal organs and tissues. It is apparent that ^{111}In-HEHEHE-Z08698-NOTA cleared more rapidly from blood but had a higher uptake in liver and spleen. Specifically, the two phenomena may be connected and elevated hepatic uptake may be a reason for more rapid conjugate elimination from blood. Furthermore, the HER3-binding site of the tested conjugates may be involved in off-target interactions and thereby influence their biodistribution profiles. The only differences between these affibody molecules in the binding sites were that Q11 and W25 in Z08698 were substituted by N11 and Y25 in Z08699. Previous findings on HER2-targeting affibody molecules (20) have shown that substitution of two amino acids in the binding site by two more lipophilic ones can cause higher hepatic uptake. Overall, ^{111}In-HEHEHE-Z08698-NOTA provided higher tumor-to-blood ratio, and should be considered as superior.

In a previous study, we evaluated targeting of BT-474 xenografts using HEHEHE-Z08699 labeled with $^{99m}Tc(CO)_3$ (4 h p.i.) (13). A comparison with ^{111}In-HEHEHE-Z08699-NOTA suggests that the combination of ^{111}In as a label and NOTA as a chelator provided a marked increase in tumor uptake (5±1 vs. 1.7±0.7 %IA/g, for ^{111}In-HEHEHE-Z08699-NOTA and $^{99m}Tc(CO)_3$-HEHEHE-Z08699, respectively). ^{111}In-HEHEHE-Z08699-NOTA provided ~2-fold higher tumor-to-stomach and tumor-to-lung ratios, the latter of which is important in the context of breast cancer as lung metastases are extremely common in this disease. This finding suggests that the HEHEHE-containing NOTA-conjugated affibody molecule is a preferable platform for further development of HER3-imaging agents.

Few studies are available on the development of imaging agents visualizing HER3 *in vivo*. One potential agent, ^{111}In-DTPA-HRG provided a tumor uptake of 2.1±0.4 %IA/g, and a tumor-to-blood ratio of 7 at 2 days p.i. in mice bearing HER3-positive xenografts (25). An anti-HER3 antibody (^{89}Zr-RG7116) demonstrated the highest tumor uptake and imaging contrast at 6 days p.i. (10). Another PET imaging probe based on a F(ab')2 antibody fragment was presented in an abstract (11). This probe demonstrated comparable contrast to the anti-HER3 affibody molecules shown in the present study, although the time point was not specified (11).

^{111}In-HEHEHE-Z08698-NOTA has reasonable imaging contrast (tumor-to-blood ratio of 12±3, tumor-to-muscle ratio of 16±4, tumor-to-lung ratio of 2.3±0.3, and tumor-to-bone ratio of 8.9±0.5) already at 4 h p.i. This indicates that this variant labeled with short-lived ^{68}Ga (T½ =67.6 min) and ^{18}F (T½ =110 min) may be useful for imaging using PET. The labeling chemistry should be re-optimized, and imaging properties have to be re-evaluated for these conjugates. However, the current study provides a good rationale for future studies.

The suggested imaging agent may enable a non-invasive and repeatable visualization of HER3 expression in metastatic cancer. Detection of HER3 overexpression onset suggests including anti-HER3 therapy to the treatment of disseminated cancer. Use of HER3-imaging agents in combination with

^{18}F-FDG PET may initially detect metastases and provide their anatomical location prior to imaging of HER3 using affibody molecules, as has been described for HER2-imaging affibody molecules.

In conclusion, ^{111}In-HEHEHE-Z08698-NOTA is a promising imaging agent for visualization of HER3-expression in cancer metastasis using SPECT. A good imaging contrast at 4 h after injection indicates that this conjugate may be used for patient stratification for anti-HER3 therapy.

Acknowledgements

The present study was supported by grants from the Swedish Cancer Society (Cancerfonden) and Swedish Research Council (Vetenskapsrådet).

References

1. Baselga J and Swain SM: Novel anticancer targets: Revisiting ERBB2 and discovering ERBB3. Nat Rev Cancer 9: 463-475, 2009.
2. Lipton A, Goodman L, Leitzel K, Cook J, Sperinde J, Haddad M, Köstler WJ, Huang W, Weidler JM, Ali S, *et al*: HER3, p95HER2, and HER2 protein expression levels define multiple subtypes of HER2-positive metastatic breast cancer. Breast Cancer Res Treat 141: 43-53, 2013.
3. Aurisicchio L, Marra E, Roscilli G, Mancini R and Ciliberto G: The promise of anti-ErbB3 monoclonals as new cancer therapeutics. Oncotarget 3: 744-758, 2012.
4. Yarden Y and Sliwkowski MX: Untangling the ErbB signalling network. Nat Rev Mol Cell Biol 2: 127-137, 2001.
5. Sergina NV, Rausch M, Wang D, Blair J, Hann B, Shokat KM and Moasser MM: Escape from HER-family tyrosine kinase inhibitor therapy by the kinase-inactive HER3. Nature 445: 437-441, 2007.
6. Kruser TJ and Wheeler DL: Mechanisms of resistance to HER family targeting antibodies. Exp Cell Res 316: 1083-1100, 2010.
7. Hamburger AW: The role of ErbB3 and its binding partners in breast cancer progression and resistance to hormone and tyrosine kinase directed therapies. J Mammary Gland Biol Neoplasia 13: 225-233, 2008.
8. Wu Y, Zhang Y, Wang M, Li Q, Qu Z, Shi V, Kraft P, Kim S, Gao Y, Pak J, *et al*: Downregulation of HER3 by a novel antisense oligonucleotide, EZN-3920, improves the antitumor activity of EGFR and HER2 tyrosine kinase inhibitors in animal models. Mol Cancer Ther 12: 427-437, 2013.
9. Malm M, Kronqvist N, Lindberg H, Gudmundsdotter L, Bass T, Frejd FY, Höidén-Guthenberg I, Varasteh Z, Orlova A, Tolmachev V, *et al*: Inhibiting HER3-mediated tumor cell growth with affibody molecules engineered to low picomolar affinity by position-directed error-prone PCR-like diversification. PLoS One 8: e62791, 2013.
10. Terwisscha van Scheltinga AG, Lub-de Hooge MN, Abiraj K, Schröder CP, Pot L, Bossenmaier B, Thomas M, Hölzlwimmer G, Friess T, Kosterink JG, *et al*: ImmunoPET and biodistribution with human epidermal growth factor receptor 3 targeting antibody ^{89}Zr-RG7116. MAbs 6: 1051-1058, 2014.
11. Wehrenberg-Klee E, Turker NS, Chang B, Heidari P and Mahmood U: Development of a HER3 PET probe for breast cancer imaging. J Nucl Med 55 (Suppl 1): s550, 2014.
12. Wester HJ and Kessler H: Molecular targeting with peptides or peptide-polymer conjugates: Just a question of size? J Nucl Med 46: 1940-1945, 2005.
13. Orlova A, Malm M, Rosestedt M, Varasteh Z, Andersson K, Selvaraju RK, Altai M, Honarvar H, Strand J, Ståhl S, *et al*: Imaging of HER3-expressing xenografts in mice using a ^{99m}Tc(CO)$_3$-HEHEHE-Z$_{HER3:08699}$ affibody molecule. Eur J Nucl Med Mol Imaging 41: 1450-1459, 2014.
14. Löfblom J, Feldwisch J, Tolmachev V, Carlsson J, Ståhl S and Frejd FY: Affibody molecules: Engineered proteins for therapeutic, diagnostic and biotechnological applications. FEBS Lett 584: 2670-2680, 2010.
15. Baum RP, Prasad V, Müller D, Schuchardt C, Orlova A, Wennborg A, Tolmachev V and Feldwisch J: Molecular imaging of HER2-expressing malignant tumors in breast cancer patients using synthetic ^{111}In- or ^{68}Ga-labeled affibody molecules. J Nucl Med 51: 892-897, 2010.
16. Sörensen J, Sandberg D, Sandström M, Wennborg A, Feldwisch J, Tolmachev V, Åström G, Lubberink M, Garske-Román U, Carlsson J, *et al*: First-in-human molecular imaging of HER2 expression in breast cancer metastases using the ^{111}In-ABY-025 affibody molecule. J Nucl Med 55: 730-735, 2014.
17. Tolmachev V, Altai M, Sandström M, Perols A, Karlström AE, Boschetti F and Orlova A: Evaluation of a maleimido derivative of NOTA for site-specific labeling of affibody molecules. Bioconjug Chem 22: 894-902, 2011.
18. Ahlgren S, Orlova A, Rosik D, Sandström M, Sjöberg A, Baastrup B, Widmark O, Fant G, Feldwisch J and Tolmachev V: Evaluation of maleimide derivative of DOTA for site-specific labeling of recombinant affibody molecules. Bioconjug Chem 19: 235-243, 2008.
19. Hofstrom C, Orlova A, Altai M, Wangsell F, Graslund T and Tolmachev V: Use of a HEHEHE purification tag instead of a hexahistidine tag improves biodistribution of affibody molecules site-specifically labeled with ^{99m}Tc, ^{111}In, and ^{125}I. J Med Chem 54: 3817-3826, 2011.
20. Tolmachev V, Tran TA, Rosik D, Sjöberg A, Abrahmsén L and Orlova A: Tumor targeting using affibody molecules: Interplay of affinity, target expression level, and binding site composition. J Nucl Med 53: 953-960, 2012.
21. Orlova A, Hofström C, Strand J, Varasteh Z, Sandstrom M, Andersson K, Tolmachev V and Gräslund T: [^{99m}Tc(CO)$_3$]$^+$-(HE)$_3$-Z$_{IGF1R:4551}$, a new Affibody conjugate for visualization of insulin-like growth factor-1 receptor expression in malignant tumours. Eur J Nucl Med Mol Imaging 40: 439-449, 2013.
22. Heskamp S, Laverman P, Rosik D, Boschetti F, van der Graaf WT, Oyen WJ, van Laarhoven HW, Tolmachev V and Boerman OC: Imaging of human epidermal growth factor receptor type 2 expression with ^{18}F-labeled affibody molecule Z$_{HER2:2395}$ in a mouse model for ovarian cancer. J Nucl Med 53: 146-153, 2012.
23. Björke H and Andersson K: Measuring the affinity of a radioligand with its receptor using a rotating cell dish with in situ reference area. Appl Radiat Isot 64: 32-37, 2006.
24. Wållberg H and Orlova A: Slow internalization of anti-HER2 synthetic affibody monomer ^{111}In-DOTA-Z$_{HER2:342-pep2}$: implications for development of labeled tracers. Cancer Biother Radiopharm 23: 435-442, 2008.
25. Razumienko EJ, Scollard DA and Reilly RM: Small-animal SPECT/CT of HER2 and HER3 expression in tumor xenografts in athymic mice using trastuzumab Fab-heregulin bispecific radioimmunoconjugates. J Nucl Med 53: 1943-1950, 2012.